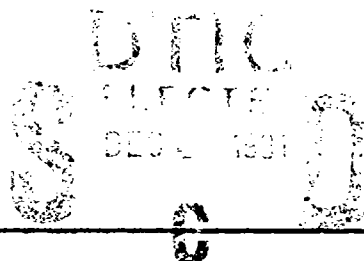


AD-A243 180



TECHNICAL REPORT BRL-TR-3295

**BRL**

LASER-BASED IGNITION OF  $H_2/O_2$  AND  $D_2/O_2$   
PREMIXED GASES NEAR 243 NM:  
THE FIRST REPORT OF A DEUTERIUM ISOTOPE  
WAVELENGTH EFFECT IN LASER IGNITION

BRAD E. FORCH  
ANDRZEJ W. MIZIOLEK

DECEMBER 1991

  
91-16948

APPROVED FOR PUBLIC RELEASE; DISTRIBUTION IS UNLIMITED.

U.S. ARMY LABORATORY COMMAND

BALLISTIC RESEARCH LABORATORY  
ABERDEEN PROVING GROUND, MARYLAND

## NOTICES

Destroy this report when it is no longer needed. DO NOT return it to the originator.

Additional copies of this report may be obtained from the National Technical Information Service, U.S. Department of Commerce, 5285 Port Royal Road, Springfield, VA 22161.

The findings of this report are not to be construed as an official Department of the Army position, unless so designated by other authorized documents.

The use of trade names or manufacturers' names in this report does not constitute indorsement of any commercial product.

# UNCLASSIFIED

REPORT DOCUMENTATION PAGE			Form Approved OMB No. 0704-0188	
Public reporting burden for this collection of information is estimated to average 1 hour per response, including the time for reviewing instructions, searching existing data sources, gathering and maintaining the data needed, and completing and reviewing the collection of information. Send comments regarding this burden estimate or any other aspect of this collection of information, including suggestions for reducing this burden, to Washington Headquarters Services, Directorate for Information Operations and Reports, 1215 Jefferson Davis Highway, Suite 1204, Arlington, VA 22202-4302, and to the Office of Management and Budget, Paperwork Reduction Project (0704-0188), Washington, DC 20503.				
1. AGENCY USE ONLY (Leave blank)	2. REPORT DATE December 1991	3. REPORT TYPE AND DATES COVERED Final, Jan 90 - Dec 90		
4. TITLE AND SUBTITLE Laser-Based Ignition of H <sub>2</sub> /O <sub>2</sub> and D <sub>2</sub> /O <sub>2</sub> Premixed Gases Near 243 nm: The First Report of a Deuterium Isotope Wavelength Effect in Laser Ignition			5. FUNDING NUMBERS  PR: AFOSR-MIPR-91-0004	
6. AUTHOR(S)  Brad E. Forch and Andrzej W. Miziolek				
7. PERFORMING ORGANIZATION NAME(S) AND ADDRESS(ES)			8. PERFORMING ORGANIZATION REPORT NUMBER	
9. SPONSORING / MONITORING AGENCY NAME(S) AND ADDRESS(ES)  U.S. Army Ballistic Research Laboratory ATTN: SLCBR-DD-T Aberdeen Proving Ground, MD 21005-5066			10. SPONSORING / MONITORING AGENCY REPORT NUMBER  BRL-TR-3295	
11. SUPPLEMENTARY NOTES				
12a. DISTRIBUTION / AVAILABILITY STATEMENT  Approved for public release; distribution is unlimited.			12b. DISTRIBUTION CODE	
13. ABSTRACT (Maximum 200 words)  We have investigated the use of a tunable laser system which operates in the ultraviolet (uv) to ignite premixed reactive gaseous flows of H <sub>2</sub> /O <sub>2</sub> and D <sub>2</sub> /O <sub>2</sub> at atmospheric pressure. The amount of incident laser energy (ILE) required to ignite the premixed flows as a function of laser excitation wavelength show two distinct minima. The spectral position of these minima correspond exactly to the location of the resonance, two-photon excitation wavelengths of atomic hydrogen and deuterium at 243.07 and 243.00 nm respectively. The relative spacing between these minima at the energy level of the 1S-2S two-photon excited transition is 22 cm <sup>-1</sup> which is in excellent agreement with the known value for H-D deuterium isotope shift (22.4 cm <sup>-1</sup> ). We believe that this is both the first report of a sensitive wavelength dependence on the laser energy required to ignite these mixtures through resonant multiphoton excitation of H and D atoms (produced from H <sub>2</sub> and D <sub>2</sub> photolysis) and the first report of a deuterium isotope-wavelength-effect in laser ignition. Measurement of the ILE required for ignition vs. equivalence ratio (Φ) shows that the most efficient ignition occurred with ~0.55 mJ ILE at Φ=0.7 in the fuel lean region.				
14. SUBJECT TERMS  Laser; ignition; hydrogen; oxygen			15. NUMBER OF PAGES 28	
			16. PRICE CODE	
17. SECURITY CLASSIFICATION OF REPORT UNCLASSIFIED	18. SECURITY CLASSIFICATION OF THIS PAGE UNCLASSIFIED	19. SECURITY CLASSIFICATION OF ABSTRACT UNCLASSIFIED	20. LIMITATION OF ABSTRACT UL	

NSN 7540-01-280-5500

## UNCLASSIFIED

Standard Form 298 (Rev. 2-89)  
Prescribed by ANSI Std. Z39-18  
298-102

INTENTIONALLY LEFT BLANK.

# TABLE OF CONTENTS

	<u>Page</u>
LIST OF FIGURES .....	v
ACKNOWLEDGMENTS .....	vii
1. INTRODUCTION .....	1
2. EXPERIMENTAL .....	3
3. RESULTS AND DISCUSSION .....	5
3.1 Microplasma Formation .....	5
3.2 Laser Power Dependencies .....	9
3.3 Ignition Experiments .....	11
4. CONCLUSION .....	14
5. REFERENCES .....	17
DISTRIBUTION LIST .....	19

Approved For	
1.1. GSAAI	<input checked="" type="checkbox"/>
1.2. IAB	<input type="checkbox"/>
1.3. Approved	<input type="checkbox"/>
Classification	
3.	
Distribution/	
Availability	
Availability/	
List	
Special	
A-1	



INTENTIONALLY LEFT BLANK.

## LIST OF FIGURES

<u>Figure</u>	<u>Page</u>
1. Schematic of Experimental Apparatus .....	4
2. Simple Energy Level Diagram for Atomic Hydrogen. Schemes 1-5 Depict Various Laser-Based Multiphoton Processes for Excitation and Ionization of the H Atom .....	6
3. Excitation Wavelength Scans for Microplasma Formation Near 243 nm With the Laser Beam Focused (ILE~1.2 mJ) Into Cold Flows of: (a) H <sub>2</sub> , $\lambda$ obs. = 656.3 nm and (b) D <sub>2</sub> , $\lambda$ obs. = 656.1 nm. The Wavelength Separation Between Peaks Is 11 cm <sup>-1</sup> Which Corresponds to 22 cm <sup>-1</sup> at the Two-Photon Excitation Energy Which Is Identical With the H-D Deuterium Isotope Shift ..	6
4. Time Resolved Emission From (a) Scattered Laser Radiation and (b) H-Atom Emission at 656.3 nm From Microplasmas Formed in H <sub>2</sub> Flows, Using Scheme 1. Figure 2, ILE = 1.2mJ .....	8
5. Excitation Wavelength Scans for Microplasma Formation Near 243 nm Plotted as a Function of ILE: (a) 0.15 mJ, (b) 0.43 mJ, (c) 0.73 mJ, and (d) 1.4 mJ in at 300 K in an Atmospheric Pressure Flow .....	8
6. Excitation Spectra of H <sup>+</sup> and D <sup>+</sup> Taken in a Time-of-Flight Mass Spectrometer Using Resonance Two-Photon Excitation and Three-Photon Ionization (2+1) of H and D Atoms Near 243 nm. The Wavelength Separation Between Peaks Is 11 cm <sup>-1</sup> Which Corresponds to 22 cm <sup>-1</sup> at the Two-Photon Excitation Energy Which Is Identical With the H-D Deuterium Isotope Shift ..	10
7. ILE Necessary to Ignite Premixed Flows of: (a) H <sub>2</sub> /O <sub>2</sub> and (b) D <sub>2</sub> /O <sub>2</sub> , as a Function of Excitation Wavelength Near 243 nm. A Shift of +11 cm <sup>-1</sup> of Ignition Curve b Relative to Ignition Curve a Is Evident .....	12
8. Dependence of the ILE Required to Ignite Premixed Flows of: (a) H <sub>2</sub> /O <sub>2</sub> and (b) D <sub>2</sub> /O <sub>2</sub> , as a Function of Equivalence Ratio. The Laser Was Set at the Peak of the Two-Photon Excitation Wavelength of: (a) H Atoms at 243.07 and (b) D Atoms at 243.00 .....	13

INTENTIONALLY LEFT BLANK.



## ACKNOWLEDGMENTS

This work was supported in part by the Air Force Office of Scientific Research (AFOSR), Directorate of Aerospace Sciences, Contract Numbers 88-0013, 89-0017 and in-house laboratory research funding (ILIR).

INTENTIONALLY LEFT BLANK.

## 1. INTRODUCTION

The use of lasers to initiate combustion events in reactive gaseous mixtures has been the subject of recent investigations in many laboratories (Forch and Miziolek 1986, 1987; Syage et al. 1988; Lavid and Stevens 1985; Raffel, Warntaz, and Wolfrum 1985). Laser ignition has generally been achieved through photochemical initiation (combustion initiation through chain-branching chemical reactions), thermal heating (laser heating of gases), nonresonant spark formation (which results from gas breakdown by intense laser radiation), and through the resonant multiphoton photochemical formation of microplasmas. Laser-induced gas breakdown, which is defined as the point in which single ionization of the gas occurs, results from the absorption of many photons which leads to ionization, collision-induced cascade ionization, and spark formation. It has been shown, however, that the laser energy at the threshold of nonresonant gas breakdown is typically far in excess of the requisite minimum ignition energy such that the formation of a blast wave may lead to a detonation (Weinberg and Wilson 1971). Here, nonresonant gas breakdown refers to spark formation in a gas which is initially transparent (early on in the laser pulse) at a particular laser wavelength. At sufficiently high field strength and as the laser pulse increases in time, electrons can be generated from multiphoton ionization of the parent fuel and/or oxidizer molecule. Electrons can then absorb radiation from the intense laser field, ionize other gas molecules, and eventually lead to cascade ionization and gas breakdown. It naturally follows that the laser energy at the sharp gas breakdown threshold may indeed exceed the minimum energy required to ignite the gas mixture and thus the extraction of a minimum ignition energy from this experiment may be difficult. However, if the laser energy threshold for the photoproduction of free electrons can be reduced (and thus electrons are produced early on in the laser pulse) then laser spark ignition may be a more controllable process. The efficient formation and characterization of laser produced sparks (microplasmas) as an ignition source is the subject of this paper.

The resonant multiphoton photochemical formation of microplasmas, which is an ignition means that we have been investigating at the Ballistic Research Laboratory, appears to be a more controllable means to generate laser-produced sparks than gas breakdown. Recent investigations (Forch and Miziolek 1986, 1987) have revealed the first example of a strong wavelength dependence in the amount of incident laser energy which was required to ignite a

premixed flow of  $\text{H}_2/\text{O}_2$  at atmospheric pressure. A tunable ultraviolet (UV) laser system which operates near 225.6 nm was found to induce photodissociation of the oxidizer component,  $\text{O}_2$  or  $\text{N}_2\text{O}$ , to produce oxygen (O) atoms in three ground-electronic spin-orbit split states  $2p^4\ ^3P_{2,1,0}$ . It was found that the minima in a plot of incident laser energy (ILE) required for ignition vs. wavelength were located exactly at the same spectral positions as the oxygen atom two-photon allowed absorption transitions from the  $2p^4\ ^3P_{2,1,0}$  states to the lowest excited state of the same symmetry (Alden et al. 1982; Miziolek and DeWilde 1984; Meier, Kohse-Hoinghaus, and Just 1986; Goldsmith 1983; Dagdigian, Forch, and Miziolek 1988). Subsequent detailed experimental investigations (Forch and Miziolek 1986, 1987) resulted in the formulation of a mechanism for this process which consists of three components: (1) the multiphoton photochemical formation of oxygen atoms; (2) resonant multiphoton ionization of these atoms to efficiently form free electrons in the laser focal volume early in the laser pulse; (3) and the controlled, resonance-enhanced formation of a microplasma using seed electrons which were generated in the previous process.

This ignition method appears to alleviate the problems associated with the sharp and uncontrolled ignition thresholds which are encountered in the extraction of minimum ignition energy measurements using desirable short-pulse lasers ( $10^{-9}$  sec) (where energy release occurs within a very short time, over a very small volume in free space and is not associated with catalytic and intrusive effects of electrode surfaces). Therefore, we began a detailed experimental investigation of the potential photochemical interaction of the UV laser and the fuel components of these premixed flows. In this paper, we describe a sensitive wavelength dependence on the laser energy required to ignite a premixed gaseous flow of  $\text{H}_2/\text{O}_2$  and  $\text{D}_2/\text{O}_2$  through resonant multiphoton excitation of hydrogen (H) and deuterium (D) atoms near 243 nm. We show that there is a definitive excitation wavelength shift near 243 nm ( $11\text{ cm}^{-1}$  at the single photon wavelength, 243 nm) for the resonant formation of microplasmas that corresponds exactly to H-D deuterium isotope shift of  $22\text{ cm}^{-1}$  at the two-photon excitation energy (two photons at 143 nm). (D is excited at a wavelength  $11\text{ cm}^{-1}$  to the blue of H and the 2S level of D is  $22\text{ cm}^{-1}$  higher in energy than the 2S level of H). Plots of ILE vs. equivalence ratio,  $\Phi$ , with the excitation wavelength of the laser tuned to either the H or D-atom two-photon transition, shows a minimum at  $\Phi = 0.7$  in the fuel lean region at an ILE of  $\sim 0.55\text{ mJ}$ . Characterization of the photochemistry involved in microplasma formation was

made. A pressure threshold for microplasma formation was determined, and an estimate of the laser power dependence for the ionization process was made.

## 2. EXPERIMENTAL

A schematic of the experimental apparatus that was used in this investigation is given in Figure 1. Tunable laser radiation near 243 nm was generated by using the second harmonic (532 nm) of a Q-switched Quanta-Ray Nd:YAG laser (DCR-2A,) to pump a Quanta-Ray Dye laser (PDL-1) which was operated at ~580 nm with a DCM dye. The dye laser beam was then frequency doubled using an angle-cut KDP crystal in the first stage of a servo-motor based tracking system, Quanta-Ray WEX-1; then the doubled radiation was frequency mixed with the 1.061 fundamental from the Nd:YAG in an angle-cut KDP crystal which was contained in the second-stage, WEX-1 module. The 243 nm laser radiation was separated from unwanted beams with two Pellin-Broca prisms (which were positioned to avoid net beam-steering), a broad-band pass filter and aperture. This configuration yielded 7-nsec (10 Hz),  $\sim 2.0 \text{ cm}^{-1}$  band width FWHM, 1.5-mJ tunable laser pulses.

The atmospheric pressure burner system consists of a water-cooled and argon-shrouded nozzle with a pinhole aperture (0.6 mm) that was mounted onto an x-y-z translation stage. Gas flows were controlled with Matheson (Model 620) flow meters or Tylan mass flow controllers (Model FC-280-V), which were calibrated by a GCA Precision Scientific wet test meter for  $\text{H}_2$ ,  $\text{D}_2$  and  $\text{O}_2$  flows up to 2 L/min. Linear flow velocities were in the  $10^3 \text{ cm/sec}$  range. The incident laser energy was measured just before a 50-mm focal length lens (the beam waist at the focus was about  $50 \mu$ ) with a Scientech (Model 38-0103) disc calorimeter-power-energy meter. The output laser energy could be varied by insertion of one (or more) dielectrically-coated partially transmitting filters in the beam and/or attenuation of the Nd:YAG amplifier stage gain. It was found that the beam characteristics (such as spatial and temporal profiles) were unaltered using this method.

Laser ignition measurements were made by flowing a carefully metered, homogeneous mixture of fuel and oxidizer through the burner. The beam was precisely focused  $\sim 0.5 \text{ mm}$  above the pinhole orifice, then the laser energy was adjusted until a single pulse ignited the gases and a flame stabilized on the burner surface. The flame was immediately extinguished

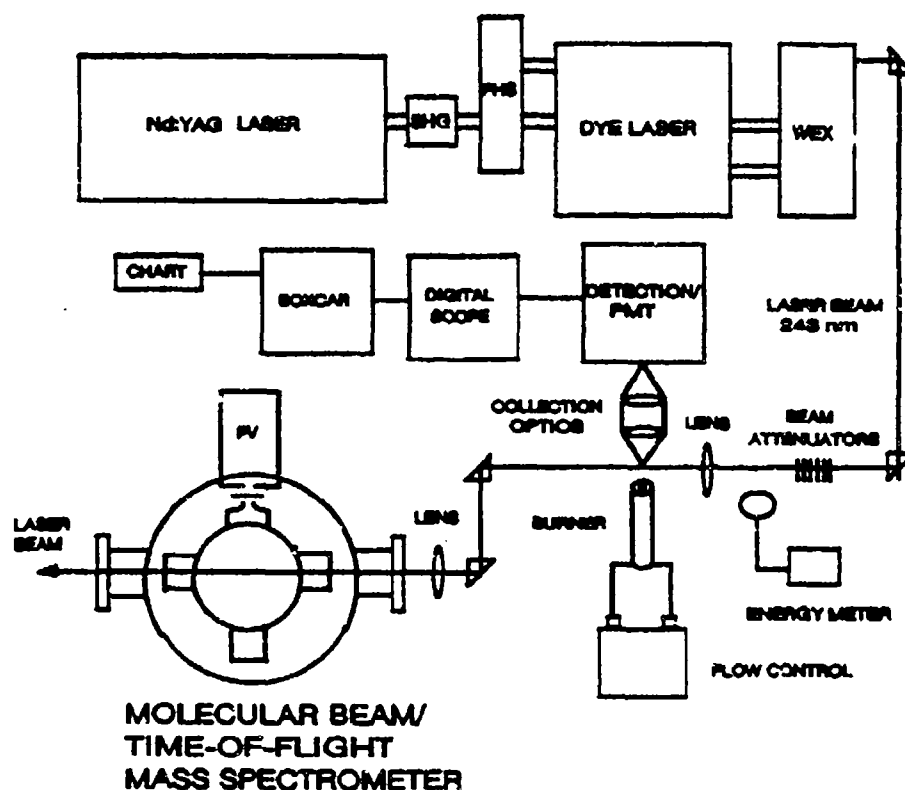


Figure 1. Schematic of Experimental Apparatus.

(fuel and oxidizer valves were closed) in order to maintain a constant burner temperature (as not to preheat the gases in succeeding measurements and to conserve the gases, especially deuterium) then the incident laser energy was measured. It was found that the measured values of ILE for ignition were independent of lateral positioning across the burner aperture (entrainment of room air in the Ar-shrouded, premixed gas jet was not occurring). Wavelength dependent ignition plots near 243 nm were generated by holding U constant and measuring ignition ILE as a function of excitation wavelength.

Excitation scans of the laser produced microplasma emission (from H or D atoms) (in cold gaseous flows or a variable pressure cell) were recorded by collecting emission (with a pair of lenses that were matched to the f/number of a 0.22-m McPherson model 180 monochromator-Hamamatsu R928 photomultiplier system). Emission signals were captured on a 500-MHz Hewlett-Packard model 54111D digital oscilloscope and/or Stanford Research Systems boxcar integrator and strip chart recorder.

Ion signals were detected in a R.M. Jordan time-of-flight mass spectrometer or using a platinum-tipped optogalvanic probe which was biased to detect free electrons liberated in the ionization process. The TOF system consists of a pulsed-molecular beam valve, a skimmed differentially pumped laser ionization region, a 1.3-m drift tube and microchannel plate detector. Operation pressure is  $\sim 10^{-7}$  Torr. The optogalvanic probe was used in atmospheric pressure gas samples. All gases were Matheson UHP and were used "as is" without further purification.

### 3. RESULTS AND DISCUSSION

**3.1 Microplasma Formation.** Figure 2 illustrates the single laser spectroscopic schemes which have been utilized for the detection of H atoms in flames, molecular beams, discharges, and other environments (Lucht et al. 1983; Alden et al. 1984; Goldsmith 1982; Goldsmith 1984; Tjossem and Cool 1983; Forch, Morris, and Miziolek 1990). The energy gap between the 1S ground electronic state and the 2S lowest excited electronic state (near-degenerate  $2S_{1/2}$ ,  $2P_{1/2}$ ,  $2P_{3/2}$  levels) is  $\sim 10$  eV (Figure 2, scheme 1). Since tunable laser sources which operate in this regime are not readily available, two-photon absorption of laser radiation at 243.07 is required to excite the 1S-2S transition. Absorption of an additional third photon from the resonantly excited 2S state is sufficient to ionize an H atom since the three-photon excitation energy ( $3 \times 5.1$  eV) exceeds the 13.6 eV H atom ionization potential. (Note that absorption of an additional photon by an H atom in any one of the excited state electronic manifolds given in Figure 2, schemes 1-5, are sufficient to achieve ionization.) Detection of laser-induced fluorescence from resonance excitation of the  $n=2$  level in flames and other environments is difficult since the emission at 122 nm is absorbed by flame and room gases. Therefore, we investigated the possibility of inducing multiphoton photolysis of  $H_2$  in a cold atmospheric flow, followed by resonance enhanced  $(2 + 1)$  multiphoton ionization H atoms to form a laser-produced microplasma. Within the high temperature plasma environment, there exist collisional processes which may populate (for example) the  $n=3$  or 4 levels where Balmer- $\beta$  (486.1 nm) or Balmer- $\alpha$  (656.3 nm) emissions could be detected (monitored by setting the monochromator at the wavelength of interest). Figure 3a gives an excitation wavelength scan where Balmer- $\beta$  emission was monitored. The signal maximum is found precisely at the known two-photon resonance transition of atomic hydrogen, although the spectral width is much larger than that of a purely atomic transition. This observation is

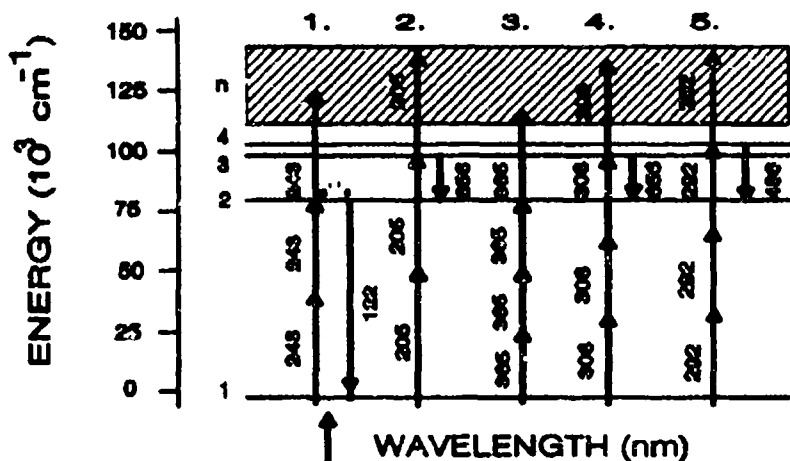


Figure 2. Simple Energy Level Diagram for Atomic Hydrogen. Schemes 1–5 Depict Various Laser-Based Multiphoton Processes for Excitation and Ionization of the H Atom.

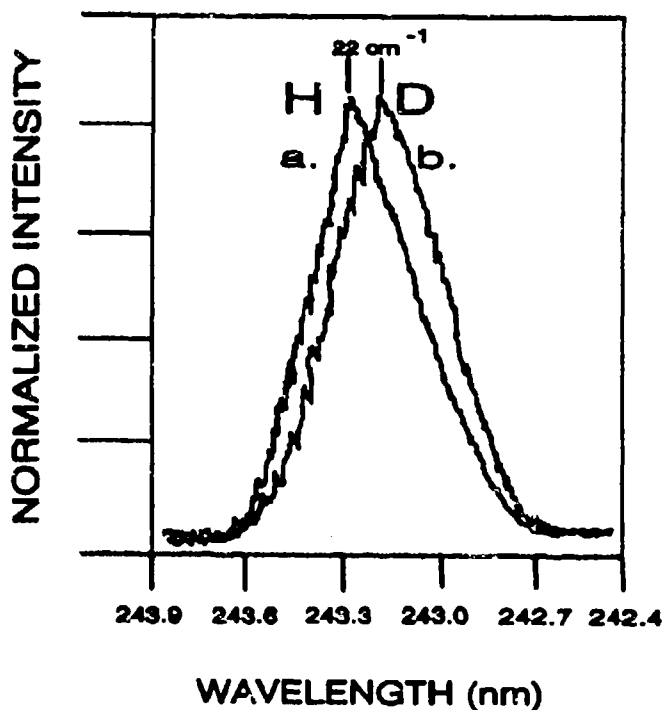


Figure 3. Excitation Wavelength Scans for Microplasma Formation Near 243 nm With the Laser Beam Focused (ILE~1.2 mJ) Into Cold Flows of: (a) H<sub>2</sub>,  $\lambda$  obs. = 656.3 nm and (b) D<sub>2</sub>,  $\lambda$  obs. = 656.1 nm. The Wavelength Separation Between Peaks Is 11  $\text{cm}^{-1}$  Which Corresponds to 22  $\text{cm}^{-1}$  at the Two-photon Excitation Energy Which Is Identical With the H-D Deuterium Isotope Shift.



clearly indicative of a much more complex, highly nonlinear phenomenon, i.e., the formation of a microplasma. Multiphoton absorption and ionization generates free electrons (priming or seed electrons) early in the laser pulse which initiate cascade ionization and the formation of a plasma which is heated up to a very high temperature by the inverse brehmsstrahlung effect.

The temporal profile of the emission, Figure 4b, is also indicative of microplasma formation. The lifetime of the emission ( $\sim 40$  ns) is much greater than that of the time-resolved scattered laser radiation ( $\sim 7$  nsec) (Figure 4a) or, for example, from resonance multiphoton laser induced fluorescence from H-atoms that we have detected using scheme 5, where the emission signal follows the temporal profile of the exciting laser pulse (Figure 4a). Although microplasma formation is initiated by atomic ionization, the lifetime of the emission is purely a property of the microplasma.

Figure 5a-d, gives the emission profiles as a function of four different laser pulse energies (0.15–1.5 mJ). The widths of the spectral profiles both increases and shows a linear dependence on laser pulse energy. Extrapolation of the measured linewidths to zero laser energy give a FWHM of  $\sim 6$   $\text{cm}^{-1}$ , which is a factor of about six times greater than the measured spectral bandwidth of the laser at this wavelength. It is known, for example, that at pressures near atmospheric the radiation intensities required to cause breakdown by the cascade processes are sufficiently strong that optically induced Stark shifts (which is a linear function of laser energy) and broadening of the electronic levels of an atom occur and have a marked influence on transition probabilities (Tjossem and Cool 1983; Lambropoulos 1974). The signals certainly are severely AC Stark broadened ( $9$   $\text{cm}^{-1}/\text{GW cm}^2$ ), however the widths are much greater than the expected natural linewidth of the atomic transition ( $\ll 1$   $\text{cm}^{-1}$ ). This evidence further indicates that emission we observe is not simply an atomic property, but that of a much more complex event.

To further verify the importance of resonance enhancement in multiphoton photochemical formation of a microplasma, these experiments were repeated under identical conditions except that  $\text{H}_2$  was replaced with  $\text{D}_2$ . Figure 3b gives the normalized spectral profile of emission signal which was observed. Note that spectra (a) and (b) are essentially identical except that the emission signal in (b) reaches a maximum at a wavelength position which is  $\sim 11$   $\text{cm}^{-1}$  to the blue of (a) (the spacing at the two-photon energy is  $\sim 22$   $\text{cm}^{-1}$ ). The

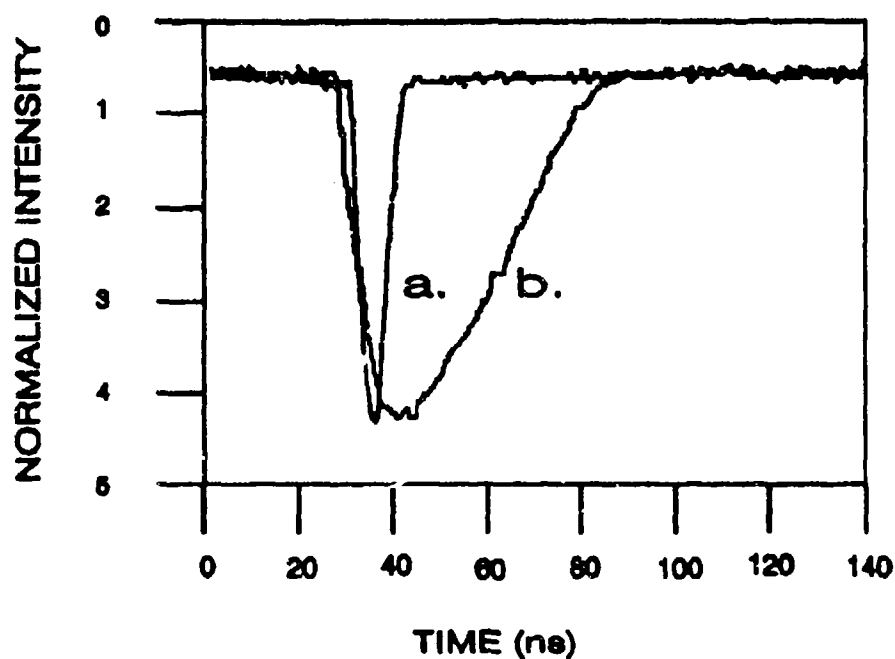


Figure 4. Time Resolved Emission From: (a) Scattered Laser Radiation and (b) H-Atom Emission at 656.3 nm: From Microplasmas Formed in H<sub>2</sub> Flows, Using Scheme 1. Figure 2, ILE = 1.2mJ.

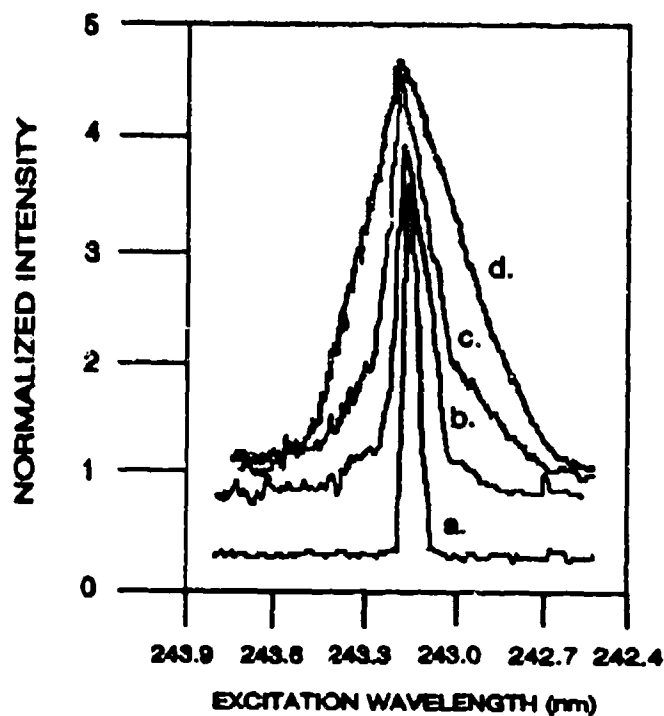


Figure 5. Excitation Wavelength Scans for Microplasma Formation Near 243 nm Plotted as a Function of ILE: (a) 0.15 mJ, (b) 0.43 mJ, (c) 0.73 mJ, and (d) 1.4 mJ in at 300 K in an Atmospheric Pressure Flow.

observation wavelength-bandpass of the monochromator was broadened and centered to equally catch both emissions at 656.3 nm and 656.1 nm for H and D, respectively. A simple calculation and check with a known value 19 shows that this separation is nearly identical with the H-D isotope shift (the D 2S level is  $22.4 \text{ cm}^{-1}$  higher in energy than the H 2S level). This isotopic shift is indeed identical to that which has been observed in spectroscopic probes of H and D atoms in flames and other environments. These results strongly support our contention that microplasma formation is the result of initial photolysis of  $\text{H}_2$  or  $\text{D}_2$  to produce ground electronic state H and D atoms and subsequent multiphoton excitation and ionization are important in the efficient wavelength dependent formation of these microplasmas, just as had been observed previously for oxidizers,  $\text{O}_2$  and  $\text{N}_2\text{O}$  (Forch and Miziolek 1986, 1987). The photoproduction of free electrons early on in the temporal evolution of the laser pulse from resonant multiphoton ionization of H or D atoms is responsible for the efficient microplasma formation. When the laser is tuned off the resonance absorption wavelengths of either H or D atoms, then no microplasma formation is seen under these experimental conditions.

**3.2 Laser Power Dependencies.** In order to gain information on the laser power dependence for the photolysis and multiphoton ionization processes, we performed a series of experiments in a well-controlled low-pressure ( $10^{-7}$  Torr) environment using a molecular-beam time-of-flight mass spectrometer (Figure 1). Curiously, we were unable to detect any  $\text{H}^+$  or  $\text{D}^+$  from laser irradiation of molecular beams of  $\text{H}_2$  or  $\text{D}_2$  when the laser beam was focused into the ionization region of the spectrometer (with the tightest focusing (200-mm f.l. lens) that geometrical constraints would allow). We did, however, find a pressure threshold of  $\sim 70$  Torr,  $\text{I}_{\text{LE}}=1.2 \text{ mJ}$ , for the onset of microplasma formation in a variable pressure flow cell. Comparison of these results suggests that a collisionally induced photodissociation process may be responsible for the production of ground state H and D atoms and subsequent microplasma formation, and, is currently under investigation. We were able to generate intense pulsed and effusive (ground state) H and D atom beams with a hot wire tungsten filament inserted before the skimmed differentially pumped ionization region in the TOF-M 20. No ions were produced from the hot wire filament itself. Ions were detected only when the laser was tuned on resonance with H and D atoms. Excitation spectra (Figure 6) were recorded by mass gating either the  $\text{H}^+$  or  $\text{D}^+$  signals with a boxcar integrator, then scanning the laser through the two-photon resonance, three photon ionization transitions (2+1) (note

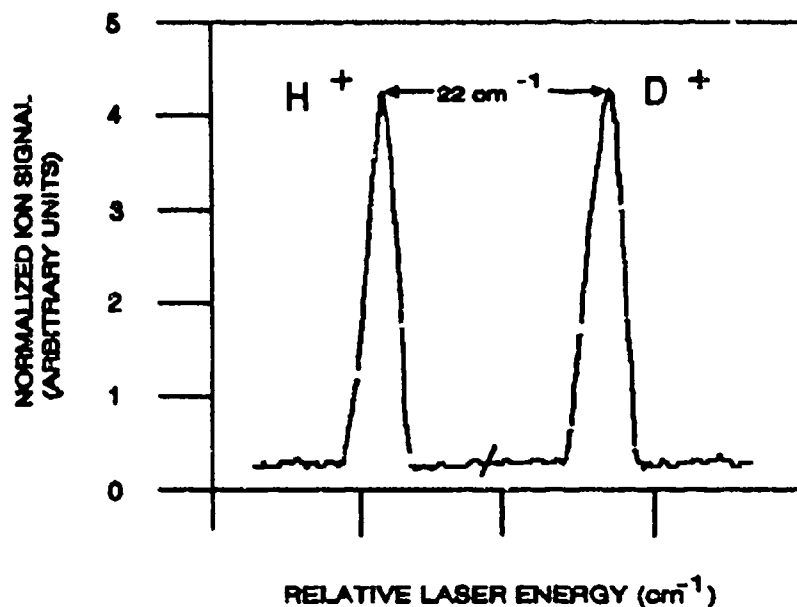


Figure 6. Excitation Spectra of  $H^+$  and  $D^+$  Taken in a Time-of-Flight Mass Spectrometer Using Resonance Two-Photon Excitation and Three-Photon Ionization (2+1) of H and D Atoms Near 243 nm. The Wavelength Separation Between Peaks Is  $11\text{ cm}^{-1}$  Which Corresponds to  $22\text{ cm}^{-1}$  at the Two-Photon Excitation Energy Which Is Identical With the H-D Deuterium Isotope Shift.

that there was virtually no signal off resonance of either excitation wavelength). Again, a wavelength spacing of  $11\text{ cm}^{-1}$  is evident, which corresponds to a deuterium isotope shift of  $22\text{ cm}^{-1}$  at the two-photon energy). Laser power dependencies for ion signal production were made assuming a signal dependence on laser intensity of  $I^n$ , where  $n$  equals the number of photons absorbed. Values of  $n=2.75\pm0.24$  and  $2.63\pm0.36$  were obtained for  $H^+$  and  $D^+$  production, respectively, which corresponds to two-photon resonance excitation and one photon ionization at low laser energies ( $<0.5\text{ mJ}$ ). These results (as expected) indicate that the overall excitation and ionization was a three-photon process. The noninteger values are indicative of partial saturation of the initial two-photon absorption and ionization step. We could easily fully saturate the ionization process at higher laser energies ( $>8.4\text{ GW/cm}^2/\text{cm}^{-1}$ ) and record laser energy dependencies of  $\sim 2$  for  $H^+$  and  $D^+$ . Although the dissociation energy of  $H_2$  is  $\sim 4.5\text{ eV}$  and the energy of a photon at  $243\text{ nm}$  is  $\sim 5.2\text{ eV}$ , absorption of a single photon is insufficient for the photoproduction of an H atom from  $H_2$  because of negligible single-photon absorption at this wavelength (the ionization potentials of  $H_2$  and  $O_2$  are  $12.06$  and  $15.43$ , respectively). Laser power dependence measurements for the photolysis of cold

flows of  $H_2$  at atmospheric pressure were made using the optogalvanic probe. The laser beam was focused  $\sim 0.5$  mm from the 1-mm-diameter anode of the probe, which was inserted in the flowing gas,  $H_2$ . Photolysis of  $H_2$  produces ground state H atoms which are photoexcited and photoionized. The liberated electrons are then detected with the optogalvanic probe. A laser power dependence measurement gave a value of  $n=4.54 \pm 0.3$ . This result also suggests a two-photon dissociation of  $H_2$  to produce H atoms. This reasoning is consistent with a two-photon dissociation of  $H_2$  to produce ground state atoms, two-photon resonance excitation and a one photon ionization. These results, when compared to the time-of-flight data and variable pressure cell data, strongly suggest a collisional induced photodissociation process may occur.

This spectroscopic data gives valuable information on the laser power dependence for microplasma formation. The overall laser energy dependence for the microplasma formation must then be at least a five photon process and clearly is highly nonlinear. The absorption of two laser photons are required for the photoproduction of ground state atoms and the absorption of three additional laser photons are necessary for photoionization. In comparison, photoproduction of atomic oxygen from molecular oxygen photodissociation near 225.6 nm gave a two-photon dependence even though the single photon energy would be sufficient for photolysis (overall a five photon process) (Forch and Miziolek 1987).

**3.3 Ignition Experiments.** We then began a series of experiments on premixed flows of  $H_2/O_2$  and  $D_2/O_2$  at atmospheric pressure in order to investigate the possibility of using these microplasmas as ignition sources. Previous work (Forch and Miziolek 1986, 1987; Syage et al. 1988; Lewis von Elbe 1951) has shown that the minimum ignition energy for these reactive gaseous mixtures occurs in the fuel lean region ( $\Phi = 0.7-0.8$ ) and is characteristic of light, diffusive fuels such as  $H_2$ , which can replenish burned fuel early on in the evolution of the ignition kernel as it expands into a stabilized flame front. In our recent work on excimer laser (ArF, 193 nm) ignition of  $H_2/O_2$  we also found that the most efficient ignition was in the fuel lean region (Forch et al. 1989). In two separate, but identical experiments, premixed flows of either  $H_2/O_2$  or  $D_2/O_2$  which were held constant at  $\Phi = 0.7$  were produced. The laser wavelength was varied and the amount of ILE required to ignite either flow into a stabilized combustion was measured. Figures 7a and 7b give the wavelength dependence on the amount of ILE necessary to ignite premixed flows of  $H_2/O_2$  and  $D_2/O_2$ , respectively. The

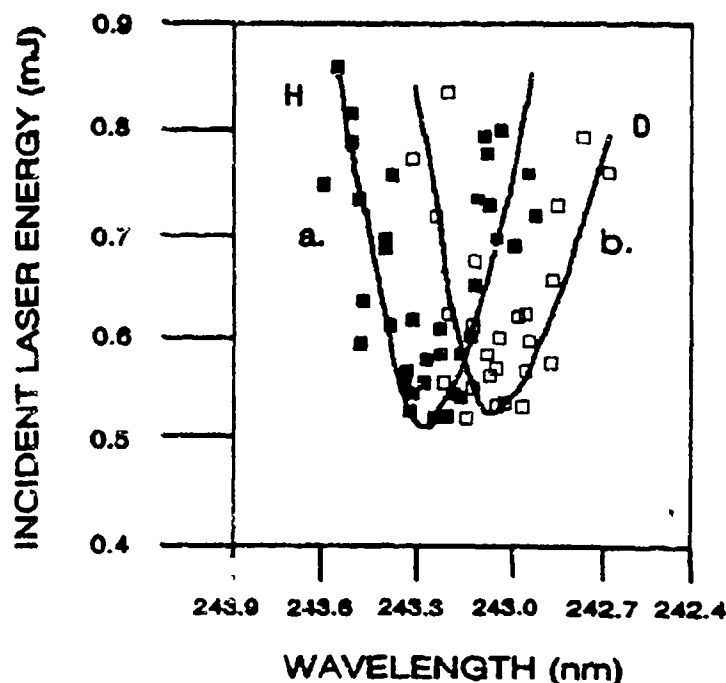


Figure 7. ILE Necessary to Ignite Premixed Flows of: (a)  $H_2/O_2$  and (b)  $D_2/O_2$ , as a Function of Excitation Wavelength Near 243 nm. A Shift of  $+11\text{ cm}^{-1}$  of Ignition Curve b Relative to Ignition Curve a Is Evident.

ignition curves clearly show a strong dependence of the ILE on the laser wavelength. Two prominent minima are evident. A simple comparison with the microplasma data (as described above) show that they correspond exactly to the spectral locations of the H and D atom two-photon resonance excitation wavelengths near 243 nm. Apparently, the focused UV laser near 243 nm not only photodissociates  $H_2$  or  $D_2$  to yield ground state atoms, but also, when on resonance with H or D, requires the least amount of laser energy to ignite the gases into a stabilized combustion. We believe that the ignition of these reactive gases occurs through the resonant formation of a microplasma from multiphoton excitation of H and D atoms. The wavelength shift of  $+11\text{ cm}^{-1}$  of the  $D_2/O_2$  ignition curve relative to that of the  $H_2/O_2$  curve is clearly related to the H-D deuterium isotope shift and underscores the importance of resonance enhancement in the ignition event. We next measured the dependence of the ILE (at a fixed laser wavelength) on  $\Phi$ . Figure 8a and b gives plots of incident laser energy required for ignition of premixed flows of  $H_2/O_2$  and  $D_2/O_2$  vs.  $\Phi$  when the laser is tuned to the two-photon resonance excitation wavelengths for H and D atoms, respectively. The observed minima in both curves occurs in the fuel lean region ( $\Phi = 0.7$ ) and with  $ILE = 0.53 \pm 0.07\text{ mJ}$  and  $0.52 \pm 0.05$  for  $H_2/O_2$  and  $D_2/O_2$ , respectively. These experiments support the three step mechanism which we have proposed which consists of the laser photoproduction of ground

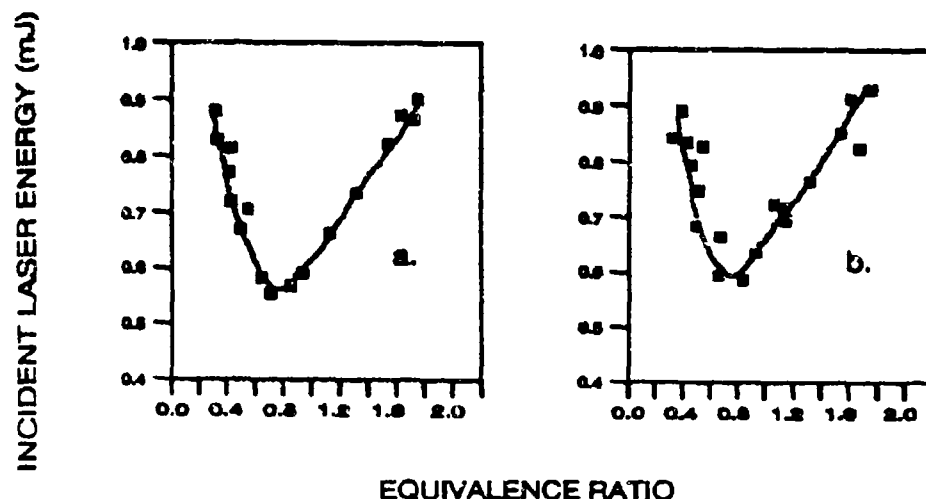


Figure 8. Dependence of the ILE Required to Ignite Premixed Flows of: (a) H<sub>2</sub>/O<sub>2</sub> and (b) D<sub>2</sub>/O<sub>2</sub>, as a Function of Equivalence Ratio. The Laser Was Set at the Peak of the Two-Photon Excitation Wavelength of: (a) H Atoms at 243.07 and (b) D Atoms at 243.00.

state atoms, resonant multiphoton ionization of the atoms to liberate free electrons early on in the laser pulse and the formation of a laser produced microplasma which serves as an ignition kernel. We have also found that microplasmas could be formed very easily through resonance multiphoton ionization, at very low laser energy, that were not intense enough to cause ignition. Thus, our method allows for precise control of laser energy in the ignition process. By comparison, we have investigated ignition of these gas mixtures using the fundamental wavelength of the same Nd:YAG laser (1064 nm) or its second harmonic (532 nm) under identical experimental conditions and found that: 1) a factor of greater than forty times more laser energy was required for ignition; 2) ignition curve plots of ILE vs.  $\Phi$  were flat (independent of  $\Phi$ ); 3) a relatively intense spark was produced. This behavior is consistent with our mechanism and reasoning. The 1064 nm and 532 nm beams are essentially initially transparent to the reactive gaseous mixture (there is no absorption of the laser light). As the laser pulse grows in intensity with time, the laser field strength reaches a point where multiphoton ionization of the fuel and/or oxidizer liberates free electrons in the laser focal volume and a very intense laser spark is produced (through nonresonant gas breakdown). Here the laser energy greatly exceeds the requisite minimum ignition energy.

Visual examination of the laser ignition sparks produced from resonant multiphoton ionization and nonresonant gas breakdown are differ dramatically the former being much less intense than the latter. This is only a qualitative observation at present, but we have purchased a high-speed streak camera to follow the temporal evolution of the laser-produced microplasmas into an ignition kernel and stabilized combustion and also perform more detailed spectroscopic examination of the sparks.) In our experiments, the incident laser energy, which is required for ignition, has been measured. Attempts to measure the energy absorbed by the microplasmas (through time-resolved absorption measurements) have been very difficult. The microplasma is heated to a very high temperature and, of course, expands with time wherein radiation losses could be significant. Furthermore, scattering of laser radiation by the microplasma occurs and has been calculated to be about 10% (Syage et al. 1988). The microplasmas are formed during the laser pulse (ca. 7 nsec) through a highly nonlinear process (at least a five photon dependence). Thus, it was very difficult to obtain reliable absorption data although recently we have successfully performed time-resolved absorption measurements on  $C_2H_2/O_2$  and  $C_2H_2/air$  ignition experiments. A rough estimate of the absorbed laser energy (making these corrections) is about 0.12 mJ at  $\Phi = 0.7$  for  $H_2/O_2$  and  $D_2/O_2$ .

#### 4. CONCLUSION

We have observed a strong wavelength dependence on the ignition of  $H_2/O_2$  and  $D_2/O_2$  premixed flows using a tunable laser near 243 nm. Furthermore, we have observed a wavelength shift in both microplasma formation in  $H_2$  and  $D_2$  gases and in the ignition of  $H_2/O_2$  and  $D_2/O_2$  flows. These results underscore the importance of two-photon atomic resonances in the microplasma formation process. We have demonstrated that our recent observations of a new laser ignition phenomenon that involves resonant multiphoton photochemical formation of microplasmas appears to be more general and applies to fuel molecules ( $H_2$  and  $D_2$ ) as well as oxidizers ( $O_2$  and  $N_2O$ ). We believe that this is the first report of a sensitive wavelength dependence on the laser energy required to ignite these mixtures through resonant multiphoton excitation of H and D atoms (produced from  $H_2$  and  $D_2$  photolysis) and the first report of a deuterium isotope effect in laser ignition. Measurement of the ILE required for ignition vs. equivalence ratio ( $\Phi$ ) shows that the most efficient ignition occurred with 0.55 mJ ILE at  $\Phi = 0.7$  in the fuel lean region. Strong experimental evidence is given which shows that ignition occurs through the resonant formation of a laser-produced



microplasma in a well-defined volume. These new experimental results indicate that resonance enhancement in the formation of a microplasma is a well controlled ignition method which appears to alleviate the problems associated with the sharp thresholds encountered in the well-known laser-produced spark (gas breakdown) process. Currently, we are exploring other possible resonance effects for the purpose of activating or enhancing the combustion of other reactive systems.

INTENTIONALLY LEFT BLANK.

## 5. REFERENCES

- Alden, M., H. Edner, P. Grafstrom, and S. Svanberg. Optics Communications. Vol. 42, p. 244, 1982.
- Alden, M., A. L. Schawlow, A. L. Svanberg, S. Wende, and P. L. Zhang. Optics Letters. Vol. 9, p. 211, 1984.
- Dagdikian, P. J., B. E. Forch, and A. W. Miziolek. Chemical Physics Letters Vol. 148, p. 299, 1988.
- Downey, S. W., and R. S. Hozack. Optics Letters. Vol. 14, p. 15, 1989.
- Forch, B. E., and A. W. Miziolek. Optics Letters. Vol. 11, p. 129, 1986.
- Forch, B. E., and A. W. Miziolek. Combustion Science and Technology. Vol. 52, p. 151, 1987.
- Forch, B. E., A. W. Miziolek, C. N. Merrow, J. B. Morris, and R. J. Locke. Proceedings of the 1989 JANNAF Combustion Meeting, The Chemical Propulsion Information Agency. Vol. 4, p. 113, October 1989.
- Forch, B. E., J. B. Morris, and A. W. Miziolek. Laser-Based Approaches in Luminescence Spectroscopy, invited book chapter, "Laser-Induced Fluorescence and Ionization Techniques in Combustion Diagnostics." Edited by T. Vo Dinh and D. Eastwood, STP 1066, p. 50, Philadelphia, 1990.
- Goldsmith, J. E. M. Optics Letters. Vol. 7, p. 437, 1982.
- Goldsmith, J. E. M. Journal of Chemical Physics. Vol. 78, p. 1610, 1983.
- Goldsmith, J. E. M. Twentieth Symposium (International) on Combustion, p. 1331, The Combustion Institute, 1984.
- Lambropoulos, P. Physics Review. Vol. 9, p. 1992, 1974.
- Lavid, M., and J. G. Stevens. Combustion and Flame. Vol. 60, p. 195, 1985.
- Lewis, B., and G. von Elbe. Combustion, Flames and Explosions of Gases. p. 390, Academic Press, Inc., 1951.
- Lucht, R. P., J. T. Salomon, G. B. King, D. W. Sweeney, and N. M. Laurendeau. Optics Letters. Vol. 8, p. 365, 1983.
- Meier, U., Th. Kohse-Hoinghaus and Just. Chemical Physics Letters. Vol. 126, p. 567, 1986.
- Miziolek, A. W., and M. A. DeWilde. Optics Letters. Vol. 9, p. 330, 1984.

- Raffei, B., B. Warntaz, and J. Wolfrum. Journal of Applied Physics. Vol. B37, p. 344, 1985.
- Striganov, A. R., and N. S. Sventitskii. Tables of Spectral Lines of Neutral and Ionized Atoms. p. 75, IFI/Plenum, 1978.
- Syage, J. A., E. W. Fournier, R. Rianda, and R. B. Cohen. Journal of Applied Physics Vol. 64, p. 1499, 1988.
- Tjossem, P. J. H., and T. A. Cool. Chemical Physics Letters. Vol. 100, p. 479, 1983.
- Weinberg, F. J., and J. R. Wilson. Proceedings of Royal Society of London Series. Vol. A321, p. 41, 1971.

<u>No. of Copies</u>	<u>Organization</u>	<u>No. of Copies</u>	<u>Organization</u>
2	Administrator Defense Technical Info Center ATTN: DTIC-DDA Cameron Station Alexandria, VA 22304-6145	1	Commander U.S. Army Missile Command ATTN: AMSMI-RD-CS-R (DOC) Redstone Arsenal, AL 35898-5010
1	Commander U.S. Army Materiel Command ATTN: AMCAM 5001 Eisenhower Avenue Alexandria, VA 22333-0001	1	Commander U.S. Army Tank-Automotive Command ATTN: ASQNC-TAC-DIT (Technical Information Center) Warren, MI 48397-5000
1	Commander U.S. Army Laboratory Command ATTN: AMSLC-DL 2800 Powder Mill Road Adelphi, MD 20783-1145	1	Director U.S. Army TRADOC Analysis Command ATTN: ATRC-WSR White Sands Missile Range, NM 88002-5502
2	Commander U.S. Army Armament Research, Development, and Engineering Center ATTN: SMCAR-IMI-I Picatinny Arsenal, NJ 07806-5000	1	Commandant U.S. Army Field Artillery School ATTN: ATSF-CSI Ft. Sill, OK 73503-5000
2	Commander U.S. Army Armament Research, Development, and Engineering Center ATTN: SMCAR-TDC Picatinny Arsenal, NJ 07806-5000	(Class. only) 1	Commandant U.S. Army Infantry School ATTN: ATSH-CD (Security Mgr.) Fort Benning, GA 31905-5660
1	Director Benet Weapons Laboratory U.S. Army Armament Research, Development, and Engineering Center ATTN: SMCAR-CCB-TL Watervliet, NY 12139-4050	(Unclass. only) 1	Commandant U.S. Army Infantry School ATTN: ATSH-CD-CSO-OR Fort Benning, GA 31905-5660
(Unclass. only) 1	Commander U.S. Army Armament, Munitions and Chemical Command ATTN: AMSMC-IMF-L Rock Island, IL 61299-5000	1	Air Force Armament Laboratory ATTN: WLMNOI Eglin AFB, FL 32542-5000
1	Director U.S. Army Aviation Research and Technology Activity ATTN: SAVRT-R (Library) M/S 219-3 Ames Research Center Moffett Field, CA 94035-1000		<u>Aberdeen Proving Ground</u>
		2	Dir, USAMSAA ATTN: AMXSY-D AMXSY-MP, H. Cohen
		1	Cdr, USATECOM ATTN: AMSTE-TC
		3	Cdr, CRDEC, AMCCOM ATTN: SMCCR-RSP-A SMCCR-MU SMCCR-MSI
		1	Dir, VLAMO ATTN: AMSLC-VL-D
		10	Dir, BRL ATTN: SLCBR-DD-T

<u>No. of</u> <u>Copies</u>	<u>Organization</u>	<u>No. of</u> <u>Copies</u>	<u>Organization</u>
1	HQDA (SARD-TR, C.H. Church) WASH DC 20310-0103	2	Commander Naval Surface Warfare Center ATTN: R. Bernecker, R-13 G.B. Wilmot, R-16 Silver Spring, MD 20903-5000
4	Commander US Army Research Office ATTN: R. Ghirardelli D. Mann R. Singleton R. Shaw P.O. Box 12211 Research Triangle Park, NC 27709-2211	5	Commander Naval Research Laboratory ATTN: M.C. Lin J. McDonald E. Oran J. Shnur R.J. Coyle, Code 6110 Washington, DC 20375
2	Commander US Army Armament Research, Development, and Engineering Center ATTN: SMCAR-AEE-B, D.S. Downs SMCAR-AEE, J.A. Lannon Picatinny Arsenal, NJ 07806-5000	1	Commanding Officer Naval Underwater Systems Center Weapons Dept. ATTN: R.S. Lazar/Code 36301 Newport, RI 02840
1	Commander US Army Armament Research, Development, and Engineering Center ATTN: SMCAR-AEE-BR, L. Harris Picatinny Arsenal, NJ 07806-5000	2	Commander Naval Weapons Center ATTN: T. Boggs, Code 388 T. Parr, Code 3895 China Lake, CA 93555-6001
2	Commander US Army Missile Command ATTN: AMSMI-RD-PR-E, A.R. Maykut AMSMI-RD-PR-P, R. Betts Redstone Arsenal, AL 35898-5249	1	Superintendent Naval Postgraduate School Dept. of Aeronautics ATTN: D.W. Netzer Monterey, CA 93940
1	Office of Naval Research Department of the Navy ATTN: R.S. Miller, Code 432 800 N. Quincy Street Arlington, VA 22217	3	AL/LSCF ATTN: R. Corley R. Geisler J. Levine Edwards AFB, CA 93523-5000
1	Commander Naval Air Systems Command ATTN: J. Ramnarace, AIR-54111C Washington, DC 20360	1	AL/MKPB ATTN: B. Goshgarian Edwards AFB, CA 93523-5000
1	Commander Naval Surface Warfare Center ATTN: J.L. East, Jr., G-23 Dahlgren, VA 22448-5000	1	AFOSR ATTN: J.M. Tishkoff Bolling Air Force Base Washington, DC 20332
		1	OSD/SDIO/IST ATTN: L. Caveny Pentagon Washington, DC 20301-7100

<u>No. of</u> <u>Copies</u>	<u>Organization</u>	<u>No. of</u> <u>Copies</u>	<u>Organization</u>
1	Commandant USAFAS ATTN: ATSF-TSM-CN Fort Sill, OK 73503-5600	1	Atlantic Research Corp. ATTN: R.H.W. Waesche 7511 Wellington Road Gainesville, VA 22065
1	F.J. Seiler ATTN: S.A. Shackelford USAF Academy, CO 80840-6528	1	AVCO Everett Research Laboratory Division ATTN: D. Stickler 2385 Revere Beach Parkway Everett, MA 02149
1	University of Dayton Research Institute ATTN: D. Campbell AL/PAP Edwards AFB, CA 93523	1	Battelle ATTN: TACTEC Library, J. Huggins 505 King Avenue Columbus, OH 43201-2693
1	NASA Langley Research Center Langley Station ATTN: G.B. Northam/MS 168 Hampton, VA 23365	1	Cohen Professional Services ATTN: N.S. Cohen 141 Channing Street Redlands, CA 92373
4	National Bureau of Standards ATTN: J. Hastie M. Jacox T. Kashiwagi H. Semerjian US Department of Commerce Washington, DC 20234	1	Exxon Research & Eng. Co. ATTN: A. Dean Route 22E Annandale, NJ 08801
1	Aerojet Solid Propulsion Co. ATTN: P. Micheli Sacramento, CA 95813	1	Ford Aerospace and Communications Corp. DIVAD Division Div. Hq., Irvine ATTN: D. Williams Main Street & Ford Road Newport Beach, CA 92663
1	Applied Combustion Technology, Inc. ATTN: A.M. Varney P.O. Box 607885 Orlando, FL 32860	1	General Applied Science Laboratories, Inc. 77 Raynor Avenue Ronkonkoma, NY 11779-6649
2	Applied Mechanics Reviews The American Society of Mechanical Engineers ATTN: R.E. White A.B. Wenzel 345 E. 47th Street New York, NY 10017	1	General Electric Ordnance Systems ATTN: J. Mandzy 100 Plastics Avenue Pittsfield, MA 01203
1	Atlantic Research Corp. ATTN: M.K. King 5390 Cherokee Avenue Alexandria, VA 22314	1	General Motors Rsch Labs Physical Chemistry Department ATTN: T. Sloane Warren, MI 48090-9055

<u>No. of Copies</u>	<u>Organization</u>
2	Hercules, Inc. Allegheny Ballistics Lab. ATTN: W.B. Walkup E.A. Yount P.O. Box 210 Rocket Center, WV 26726
1	Alliant Techsystems, Inc. Marine Systems Group ATTN: D.E. Broder/ MS MN5C-2000 600 2nd Street NE Hopkins, MN 55343
1	Alliant Techsystems, Inc. ATTN: R.E. Tompkins MN38-3300 5700 Smetana Drive Minnetonka, MN 55343
1	IBM Corporation ATTN: A.C. Tam Research Division 5600 Cottle Road San Jose, CA 95193
1	IIT Research Institute ATTN: R.F. Remaly 10 West 35th Street Chicago, IL 60616
2	Director Lawrence Livermore National Laboratory ATTN: C. Westbrook M. Costantino P.O. Box 808 Livermore, CA 94550
1	Lockheed Missiles & Space Co. ATTN: George Lo 3251 Hanover Street Dept. 52-35/B204/2 Palo Alto, CA 94304
1	Director Los Alamos National Lab ATTN: B. Nichols, T7, MS-B284 P.O. Box 1663 Los Alamos, NM 87545

<u>No. of Copies</u>	<u>Organization</u>
1	National Science Foundation ATTN: A.B. Harvey Washington, DC 20550
1	Olin Ordnance ATTN: V. McDonald, Library P.O. Box 222 St. Marks, FL 32355-0222
1	Paul Gough Associates, Inc. ATTN: P.S. Gough 1048 South Street Portsmouth, NH 03801-5423
2	Princeton Combustion Research Laboratories, Inc. ATTN: M. Summerfield N.A. Messina 475 US Highway One Monmouth Junction, NJ 08852
1	Hughes Aircraft Company ATTN: T.E. Ward 8433 Fallbrook Avenue Canoga Park, CA 91303
1	Rockwell International Corp. Rocketdyne Division ATTN: J.E. Flanagan/HB02 5633 Canoga Avenue Canoga Park, CA 91304
4	Director Sandia National Laboratories Division 8354 ATTN: R. Cattolica S. Johnston P. Mattern D. Stephenson Livermore, CA 94550
1	Science Applications, Inc. ATTN: R.B. Edelman 23146 Cumorah Crest Woodland Hills, CA 91364
3	SRI International ATTN: G. Smith D. Crosley D. Golden 333 Ravenswood Avenue Menlo Park, CA 94025



<u>No. of</u> <u>Copies</u>	<u>Organization</u>	<u>No. of</u> <u>Copies</u>	<u>Organization</u>
1	Stevens Institute of Tech. Davidson Laboratory ATTN: R. McAlevy, III Hoboken, NJ 07030	1	Brigham Young University Dept. of Chemical Engineering ATTN: M.W. Beckstead Provo, UT 84058
1	Sverdrup Technology, Inc. LERC Group ATTN: R.J. Locke, MS SVR-2 2001 Aerospace Parkway Brook Park, OH 44142	1	California Institute of Tech. Jet Propulsion Laboratory ATTN: L. Strand/MS 512/102 4800 Oak Grove Drive Pasadena, CA 91109
1	Sverdrup Technology, Inc. ATTN: J. Deur 2001 Aerospace Parkway Brook Park, OH 44142	1	California Institute of Technology ATTN: F.E.C. Culick/ MC 301-46 204 Karman Lab. Pasadena, CA 91125
1	Thiokol Corporation Elkton Division ATTN: S.F. Palopoli P.O. Box 241 Elkton, MD 21921	1	University of California Los Alamos Scientific Lab. P.O. Box 1663, Mail Stop B216 Los Alamos, NM 87545
3	Thiokol Corporation Wasatch Division ATTN: S.J. Bennett P.O. Box 524 Brigham City, UT 84302	1	University of California, Berkeley Chemistry Department ATTN: C. Bradley Moore 211 Lewis Hall Berkeley, CA 94720
1	United Technologies Research Center ATTN: A.C. Eckbreth East Hartford, CT 06108	1	University of California, San Diego ATTN: F.A. Williams AMES, B010 La Jolla, CA 92093
3	United Technologies Corp. Chemical Systems Division ATTN: R.S. Brown T.D. Myers (2 copies) P.O. Box 49028 San Jose, CA 95161-9028	2	University of California, Santa Barbara Quantum Institute ATTN: K. Schofield M. Steinberg Santa Barbara, CA 93106
1	Universal Propulsion Company ATTN: H.J. McSpadden Black Canyon Stage 1 Box 1140 Phoenix, AZ 85029	1	University of Colorado at Boulder Engineering Center ATTN: J. Daily Campus Box 427 Boulder, CO 80309-0427
1	Veritay Technology, Inc. ATTN: E.B. Fisher 4845 Millersport Highway P.O. Box 305 East Amherst, NY 14051-0305		

No. of  
Copies      Organization

2      University of Southern  
         California  
         Dept. of Chemistry  
         ATTN: S. Benson  
         C. Wittig  
         Los Angeles, CA 90007

1      Cornell University  
         Department of Chemistry  
         ATTN: T.A. Cool  
         Baker Laboratory  
         Ithaca, NY 14853

1      University of Delaware  
         ATTN: T. Brill  
         Chemistry Department  
         Newark, DE 19711

1      University of Florida  
         Dept. of Chemistry  
         ATTN: J. Winefordner  
         Gainesville, FL 32611

3      Georgia Institute of Technology  
         School of Aerospace Engineering  
         ATTN: E. Price  
         W.C. Strahle  
         B.T. Zinn  
         Atlanta, GA 30332

1      University of Illinois  
         Dept. of Mech. Eng.  
         ATTN: H. Krier  
         144MEB, 1206 W. Green St.  
         Urbana, IL 61801

1      Johns Hopkins University/APL  
         Chemical Propulsion  
         Information Agency  
         ATTN: T.W. Christian  
         Johns Hopkins Road  
         Laurel, MD 20707

1      University of Michigan  
         Gas Dynamics Lab  
         Aerospace Engineering Bldg.  
         ATTN: G.M. Faeth  
         Ann Arbor, MI 48109-2140

No. of  
Copies      Organization

1      University of Minnesota  
         Dept. of Mechanical  
         Engineering  
         ATTN: E. Fletcher  
         Minneapolis, MN 55455

3      Pennsylvania State University  
         Applied Research Laboratory  
         ATTN: K.K. Kuo  
         H. Palmer  
         M. Micci  
         University Park, PA 16802

1      Pennsylvania State University  
         Dept. of Mechanical Engineering  
         ATTN: V. Yang  
         University Park, PA 16802

1      Polytechnic Institute of NY  
         Graduate Center  
         ATTN: S. Lederman  
         Route 110  
         Farmingdale, NY 11735

2      Princeton University  
         Forrestal Campus Library  
         ATTN: K. Brezinsky  
         I. Glassman  
         P.O. Box 710  
         Princeton, NJ 08540

1      Purdue University  
         School of Aeronautics  
         and Astronautics  
         ATTN: J.R. Osborn  
         Grissom Hall  
         West Lafayette, IN 47906

1      Purdue University  
         Department of Chemistry  
         ATTN: E. Grant  
         West Lafayette, IN 47906

2      Purdue University  
         School of Mechanical  
         Engineering  
         ATTN: N.M. Laurendeau  
         S.N.B. Murthy  
         TSPC Chaffee Hall  
         West Lafayette, IN 47906

<u>No. of Copies</u>	<u>Organization</u>
1	Rensselaer Polytechnic Inst. Dept. of Chemical Engineering ATTN: A. Fortijn Troy, NY 12181
1	Stanford University Dept. of Mechanical Engineering ATTN: R. Hanson Stanford, CA 94305
1	University of Texas Dept. of Chemistry ATTN: W. Gardiner Austin, TX 78712
1	University of Utah Dept. of Chemical Engineering ATTN: G. Flandro Salt Lake City, UT 84112
1	Virginia Polytechnic Institute and State University ATTN: J.A. Schetz Blacksburg, VA 24061
1	Freedman Associates ATTN: E. Freedman 2411 Diana Road Baltimore, MD 21209-1525